

## The Hubble Space Telescope $H_0$ Key Project

Wendy L. Freedman  
*Carnegie Observatories, 813 Santa Barbara St., Pasadena, CA 91106,*  
*USA*

Robert C. Kennicutt  
*Steward Observatory, Arizona*

Jeremy R. Mould  
*Australian National University, Siding Springs, Australia*

Barry F. Madore  
*IPAC/Carnegie, Pasadena, CA*

**Abstract.** As this conference has attested to, cosmology is a rapidly maturing field, currently experiencing a very healthy and vigorous confrontation between theory and experiment. This rapid progress in many different areas of cosmology has not removed the longstanding interest in measuring many of the fundamental cosmological parameters – rather, the increasingly detailed predictions of current theory highlight the critical importance of *independently*, accurately measuring the cosmological parameters which define the basic model for the dynamical evolution of the Universe. I present here the final results of the Hubble Space Telescope (HST) Key Project to measure the Hubble constant, summarizing our method, the results and the uncertainties. The Key Project results are based on a Cepheid calibration of several secondary distance methods applied over the range of about 60 to 400 Mpc. Based on the Key Project Cepheid calibration and its application to five secondary methods (type Ia supernovae, the Tully–Fisher relation, surface brightness fluctuations, type II supernovae, and the fundamental plane for elliptical galaxies), a combined value of  $H_0 = 72 \pm 8$  km/sec/Mpc is obtained. Comparing to current estimates of the ages of Galactic globular clusters, an age conflict is avoided for this high a value of  $H_0$  if we live in a  $\Lambda$ -dominated (or other form of dark energy) universe.

### 1. Introduction

Obtaining an accurate value for the Hubble constant has proved an extremely challenging endeavor, a result primarily of the underlying difficulty of establishing accurate distances over cosmologically significant scales. The overall goal of the  $H_0$  Key Project (hereafter, Key Project) was to measure  $H_0$  based on a Cepheid calibration of a number of independent, secondary distance determination methods. Given the history of systematic errors dominating the accuracy of distance measurements, the approach adopted was to avoid relying on a single method alone, and instead to average over the systematics by calibrating and using a number of different methods. Determining  $H_0$  accurately requires the measurement of distances far enough away that both the small and large-scale

motions of galaxies become small compared to the overall Hubble expansion. To extend the distance scale beyond the range of the Cepheids, a number of methods that provide relative distances were chosen. We have used the HST Cepheid distances to provide an absolute distance scale for these otherwise independent methods, including the Type Ia supernovae (Gibson *et al* 2000), the Tully-Fisher relation (Sakai *et al* 2000), the fundamental plane for elliptical galaxies (Kelson *et al* 2000), surface-brightness fluctuations (Ferrarese *et al* 2000a), and Type II supernovae. This review is based on the results presented in more detail in a final summary of the Key Project by Freedman *et al.* (2001), which also contains a more extensive reference list. An earlier summary is given by Mould *et al.* (2000).

## 2. The $H_0$ HST Key Project

The  $H_0$  Key Project involved the dedication and hard work of an enormous number of people with a range of expertise in the Cepheid distance scale, secondary distance methods, and crowded-field photometry. Over the years, the members of the Key Project have included W. L. Freedman, R. Kennicutt, J. R. Mould (co-PI's), F. Bresolin, S. Faber, L. Ferrarese, H. Ford, J. Graham, J. Gunn, M. Han, P. Harding, R. Hill, J. Hoessel, J. Huchra, S. Hughes, G. Illingworth, D. Kelson, L. Macri, B. F. Madore, R. Phelps, D. Rawson, A. Saha, S. Sakai, K. Sebo, N. Silbermann, and P. Stetson and A. Turner.

The Key Project was designed to use Cepheid variables to determine primary distances to a representative sample of nearby galaxies in the field, groups, and clusters. The galaxies were chosen so that each of the secondary distance indicators with measured high internal precisions could be calibrated in zero point, and then intercompared on an absolute basis. The Cepheid distances were then used for secondary calibrations out to cosmologically significant distances, with a goal of measuring  $H_0$  to an accuracy of  $\pm 10\%$ , including systematic errors. The excellent image quality of HST extends the limit out to which Cepheids can be discovered by a factor of ten from ground-based searches, and the effective search volume by a factor of a thousand. Furthermore, HST offers a unique capability in that it can be scheduled optimally and independently of the phase of the Moon, the time of day, or weather, and there are no seeing variations. Before the launch of HST, most Cepheid searches were confined to our own Local Group of galaxies, and the very nearest surrounding groups, and the numbers of Cepheid calibrators for various methods was dismally small (5 for the Tully-Fisher relation, one for the surface-brightness fluctuation method, and *no* Cepheid calibrators were available for Type Ia supernovae.

In each nearby target spiral galaxy in the Key Project sample, Cepheid searches were undertaken in regions active in star formation, but low in apparent dust extinction. To the largest extent possible, we avoided high-surface-brightness regions in order to minimize source confusion or crowding. For each galaxy, over a two-month time interval, HST images in the visual (V-band, 5550 Å), and in the near-infrared (I band, 8140 Å), were made using the corrected Wide Field and Planetary Camera 2 (WFPC2). Two wavelength bands were chosen to enable corrections for dust extinction. The time distribution of the observations was set to follow a power-law, enabling the detection

and measurement of Cepheids with a range of periods optimized for minimum aliasing between 10 and 50 days. For each galaxy observed as part of the Key Project, the Cepheid positions, magnitudes, and periods are available at <http://www.ipac.caltech.edu/H0kp/H0KeyProj.html>. In addition, photometry for non-variable stars that can be used for photometry comparisons, as well as medianed (non-photometric) images for these galaxies are also available. These images are also archived in NED, and can be accessed on a galaxy-by-galaxy basis from <http://nedwww.ipac.caltech.edu>.

Since each individual secondary method is likely to be affected by its own (independent) systematic uncertainties, to reach a final overall uncertainty of  $\pm 10\%$ , the numbers of calibrating galaxies for a given method were chosen initially so that the final (statistical) uncertainty on the zero point for that method would be only  $\sim 5\%$ . Cepheid distances were obtained for 18 galaxies. These galaxies lie at distances between 3 and 25 Mpc. HST has also been used to measure Cepheid distances to 6 galaxies, targeted specifically to be useful for the calibration of Type Ia supernovae (*e.g.* Sandage *et al* 1996). Finally, an HST distance to a single galaxy in the Leo I group, NGC 3368, was measured by Tanvir and collaborators (Tanvir *et al* 1999). Subsequently and fortuitously, NGC 3368 was host to a Type Ia supernova, useful for calibrating  $H_0$  (Jha *et al* 1999). In addition, recently, SN1999by occurred in NGC 2841, a galaxy for which Cepheid observations have been taken in Cycle 9 (GO-8322).

Each galaxy within the Key Project was analyzed by two independent groups within the team: only at the end of the data reduction process (including the Cepheid selection and distance determinations) were the two groups' results intercompared. This "double-blind" procedure proved extremely valuable, both for catching simple (operator) errors, as well as enabling us to provide a more realistic estimate of the external data reduction errors for each galaxy distance. We also undertook a series of artificial star tests to better quantify the effects of crowding, and to understand the limits in each of these software packages (Ferrarese *et al.*, 2000b). The final distances were obtained by fitting each individual galaxy VI period–luminosity relations to those for the Large Magellanic Cloud (LMC) measured by Udalski *et al.* (1999), assuming a distance to the LMC of  $18.50 \pm 0.10$  mag (*rms*).

### 3. Metallicity and the Cepheid Distance Scale

Accurately establishing whether the zero point of the Cepheid period–luminosity relation sensitive to chemical composition has proven to be very challenging, and the issue has not yet been definitively resolved (see Freedman *et al.* 2001 and references therein). Neither the magnitude of the effect nor its wavelength dependence have yet been firmly established, but the observational and theoretical evidence for an effect is steadily growing. Some recent theoretical models (*e.g.*, see Alibert *et al.* 1999) suggest that at the VI bandpasses of the  $H_0$  Key Project, the effect of metallicity on the derived distance is small, amounting to only about 0.1 mag over a dex (or a factor of ten in metallicity). Unfortunately, however, the sign of the effect is still uncertain. For example, Caputo, Marconi & Musella (2000) find a slope of 0.27 mag/dex, with the opposite sign. Thus, for the present, calibrating the metallicity effect based on theoretical models

alone is not feasible. Considering all of the evidence presently available and the (still considerable) uncertainties, we adopted a metallicity correction to the Key Project distances of  $-0.2 \pm 0.2$  mag/dex, approximately the mid-range of current empirical values.

#### 4. The Hubble Constant

Calibrating 5 secondary methods with Cepheid distances, Freedman *et al.* (2001) find  $H_0 = 72 \pm 3$  (random)  $\pm 7$  (systematic) km/sec/Mpc. Type Ia supernovae are the secondary method which currently extends out to the greatest distances,  $\sim 400$  Mpc. All of the methods (Types Ia and II supernovae, the Tully–Fisher relation, surface brightness fluctuations, and the fundamental plane) are in extremely good agreement: four of the methods yield a value of  $H_0$  between 70–72 km/sec/Mpc, and the fundamental plane gives  $H_0 = 82$  km/sec/Mpc. As described in detail in Freedman *et al.*, the largest remaining sources of error result from (a) uncertainties in the distance to the Large Magellanic Cloud, (b) photometric calibration of the HST Wide Field and Planetary Camera 2, (c) metallicity calibration of the Cepheid period–luminosity relation, and (d) cosmic scatter in the density (and therefore, velocity) field that could lead to observed variations in  $H_0$  on very large scales. These systematic uncertainties affect the determination of  $H_0$  for all of the relative distance indicators, and they cannot be reduced by simply combining the results from different methods: they dominate the overall error budget in the determination of  $H_0$ .

Figure 1 shows the probability distributions for the individual  $H_0$  determinations. The median value is  $H_0 = 72 \pm 3 \pm 7$  km/sec/Mpc. A Bayesian analysis was also done assuming that the priors on  $H_0$  and on the probability of any single measurement being correct are uniform. Here the product of the probability distributions yields  $H_0 = 72 \pm 2 \pm 7$  km/sec/Mpc. The formal uncertainty on this result is very small, and simply reflects the fact that four of the values are clustered very closely, while the uncertainties in the fundamental method are large. Adjusting for differences in calibration, these results are also in excellent agreement with the weighting based on numerical simulations of the errors by Mould *et al.* (2000) which yielded  $71 \pm 6$  km/sec/Mpc similar to Madore *et al.* (1999) giving  $H_0 = 72 \pm 5 \pm 7$  km/sec/Mpc based on a smaller subset of available Cepheid calibrators. Figure 2 displays the results graphically in a composite Hubble diagram. The Hubble line plotted in this figure has a slope of 72 km/sec/Mpc.

#### 5. $H_0$ From Methods Independent of Cepheids

At present, to within the uncertainties, there is broad agreement in  $H_0$  values for completely independent techniques. Published values of  $H_0$  based on the Sunyaev–Zeldovich (SZ) method have ranged from  $\sim 40 - 80$  km/sec/Mpc (*e.g.*, Birkinshaw 1999). The most recent two-dimensional interferometry SZ data for well-observed clusters yield  $H_0 = 60 \pm 10$  km/sec/Mpc. The systematic uncertainties are still large, but the near-term prospects for this method are improving rapidly as additional clusters are being observed, and higher-resolution X-ray and SZ data are becoming available (*e.g.*, Reese *et al.* 2000). A second

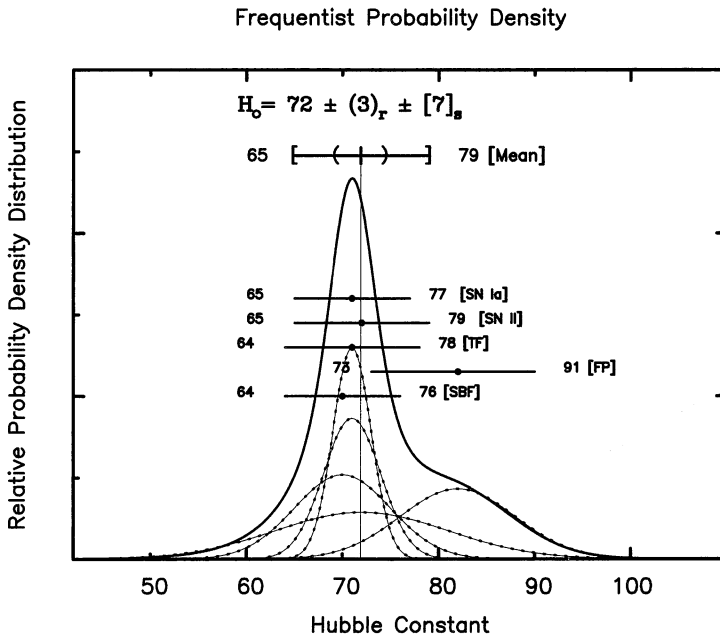


Figure 1. Probability distributions for the individual  $H_0$  determinations. Each is represented by a Gaussian of unit area, with a dispersion given by the individual  $\sigma$  values. The cumulative distribution is given by the solid thick line. The median value is  $H_0 = 72 \pm 3 \pm 7$  km/sec/Mpc. The *random* uncertainty is defined at the  $\pm 34\%$  points of the cumulative distribution.

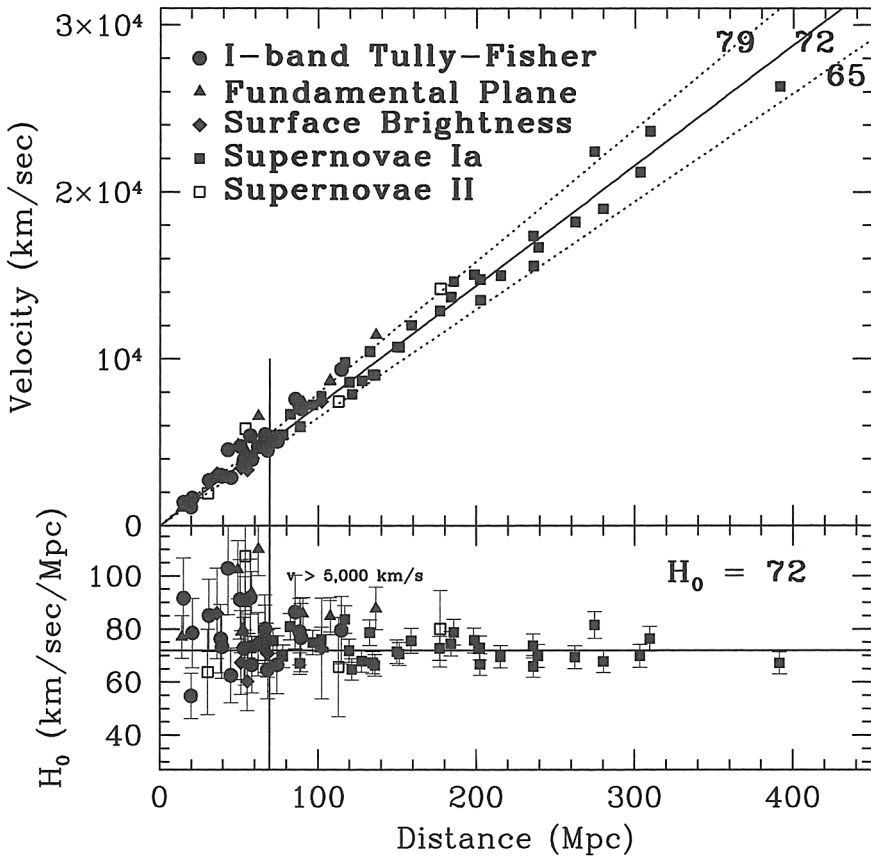


Figure 2. Composite Hubble diagram of velocity versus distance for Type Ia supernovae (solid squares), the Tully-Fisher relation (solid circles), surface-brightness fluctuations (solid diamonds), the fundamental plane (solid triangles), and Type II supernovae (open squares). In the bottom panel, the values of  $H_0$  are shown as a function of distance. The Cepheid distances have been corrected for metallicity. The Hubble line plotted in this figure has a slope of 72 km/sec/Mpc, and the adopted distance to the LMC is taken to be 50 kpc.

method for measuring  $H_0$  at very large distances, also independent of the need for any local calibration, comes from the measurement of time delays in gravitational lenses.  $H_0$  values based on this technique appear to be converging to the mid-60 km/sec/Mpc range (Williams & Saha 2000). As more lenses with time delays are discovered and monitored, this method also is likely to improve substantially in the near future. A Hubble diagram ( $\log d$  versus  $\log v$ ) is plotted in Figure 3.

## 6. The Expansion Age and Implications for Cosmology

An accurate determination of the expansion age of the universe requires not only the value of  $H_0$ , but also accurate measurements of  $\Omega_m$  and  $\Omega_\Lambda$ . At the time when the Key Project was begun, the strong motivation from inflationary theory for a flat universe, coupled with a strong theoretical preference for  $\Omega_\Lambda = 0$ , favored the Einstein-de Sitter model (*e.g.*, Kolb & Turner 1990). In addition, the ages of globular cluster stars were estimated at that time to be  $\sim 15$  Gyr (Chaboyer *et al.* 1996). However, for a value of  $H_0 = 72$  km/sec/Mpc, the Einstein-de Sitter model yields a very young expansion age of only  $9 \pm 1$  Gyr, significantly younger than the globular cluster and other age estimates. In Figure 4  $H_0 t_0$  is plotted as a function of  $\Omega$ , for a value of  $H_0 = 72$  km/sec/Mpc and  $t_0 = 12.5$  Gyr.

A non-zero value of the cosmological constant helps to avoid a discrepancy between the expansion age and other age estimates. For  $H_0 = 72$  km/sec/Mpc,  $\Omega_m = 0.3$ ,  $\Omega_\Lambda = 0.7$ , the expansion age is  $13 \pm 1$  Gyr. This age is consistent to within the uncertainties with recent globular cluster ages, which have been revised downward to 12-13 Gyr based on a new calibration from the Hipparcos satellite (Chaboyer 1998), with the evidence from recent cosmic microwave background anisotropy experiments (de Bernardis *et al.* 2000 and with recent data from high-redshift supernovae providing evidence for a non-zero cosmological constant (Riess *et al.* 1998; Perlmutter *et al.* 1999).

## 7. Summary

A ten-year HST Key Project to measure the Hubble constant has just been completed. HST was used to measure Cepheid distances to 18 nearby spiral galaxies. Calibrating 5 secondary methods with these revised Cepheid distances yields  $H_0 = 72 \pm 3$  (random)  $\pm 7$  (systematic) km/sec/Mpc, or  $H_0 = 72 \pm 8$  km/sec/Mpc, combining the total errors in quadrature. To within existing uncertainties, these results are in good agreement with other completely independent methods for measuring  $H_0$ , for example, the Sunyaev-Zeldovich and gravitational lense time delay methods. The largest remaining sources of error result from (a) uncertainties in the distance to the Large Magellanic Cloud, (b) photometric calibration of the HST Wide Field and Planetary Camera 2, (c) metallicity calibration of the Cepheid period-luminosity relation, and (d) cosmic scatter in the density (and therefore, velocity) field that could lead to observed variations in  $H_0$  on very large scales. A value of  $H_0 = 72$  km/sec/Mpc yields an expansion age of  $\sim 13$  Gyr for a flat universe (consistent with the recent cosmic microwave background anisotropy results) if  $\Omega_m = 0.3$ ,  $\Omega_\Lambda = 0.7$ . Combined



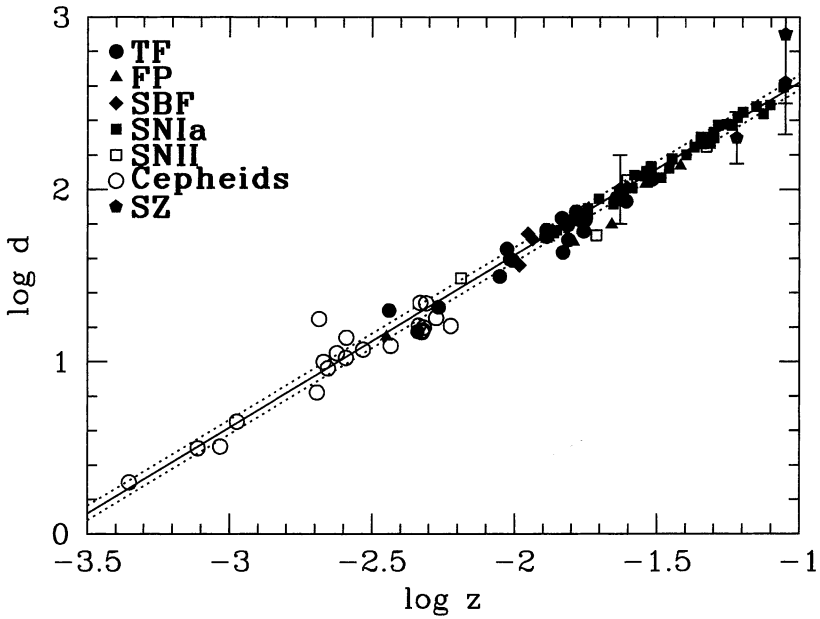


Figure 3. Hubble diagram ( $\log d$  versus  $\log v$ ) covering over 3 orders of magnitude, including distances obtained locally from Cepheids, from 5 secondary methods, and for 4 clusters with recent Sunyaev-Zel'dovich measurements out to  $z \sim 0.1$ . At redshifts beyond  $z$  of 0.1, other cosmological parameters (the matter density,  $\Omega_m$ , and the cosmological constant,  $\Omega_\Lambda$ ) become important.



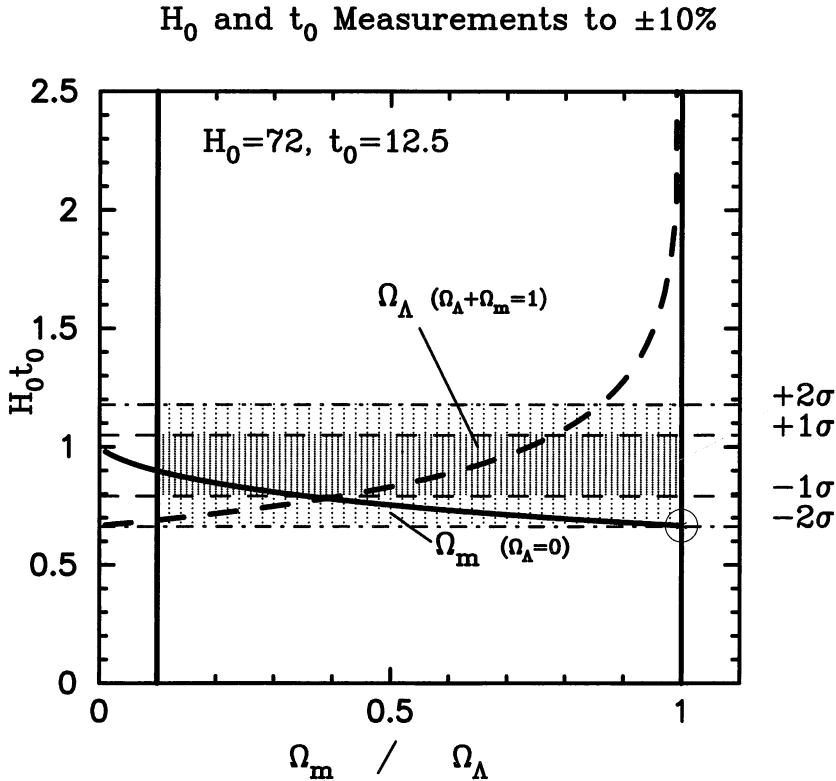


Figure 4. Plot of  $H_0 t_0$  as a function of  $\Omega$ . Two curves are shown: the solid curve is for the case where  $\Lambda = 0$ , and the dashed curve allows for non-zero  $\Lambda$  under the assumption of a flat universe. The  $\pm 1$ - and  $2$ - $\sigma$  limits are plotted for  $H_0 = 72$  km/sec/Mpc,  $t_0 = 12.5$  Gyr, assuming independent uncertainties of  $\pm 10\%$  in each quantity, and adding the uncertainties in quadrature. These data are consistent with either a low-density ( $\Omega_m \sim 0.1$ ) open universe, or a flat universe with  $\Omega_m \sim 0.35$ ,  $\Omega_\Lambda = 0.65$ ; however, with these data alone, it is not possible to discriminate between an open or flat universe. The open circle at  $\Omega_m = 1$ ,  $\Lambda = 0$ , represents the Einstein-de Sitter case, and is inconsistent with the current values of  $H_0$  and  $t_0$  only at a  $\sim 2$ - $\sigma$  level.

with the current best estimates of the ages of globular clusters ( $\sim 12.5$  Gyr), our results favor a  $\Lambda$ -dominated universe.

## References

- Alibert, Y., Baraffe, I., Hauschildt, P. and Allard, F. 1999, *A&A*, 344, 551  
Birkinshaw, M. 1999, *Phys. Rep.*, 310, 97  
Caputo, F., Marconi, M., Musella, I., & Santolamazza, P. 2000, *A & A*, 359, 1059  
Chaboyer, B., Demarque, P., Kernan, P. J., & Krauss, L. M. 1996, *Science*, 271, 957  
Chaboyer, B., Demarque, P., Kernan, P.J., & Krauss, L. M. 1998, *ApJ*, 494, 96  
de Bernardis, P. *et al.* 2000, *Nature*, 404, 955  
Ferrarese, L., *et al.* 2000a, *ApJ*, 529, 745  
Ferrarese, L., Silbermann, N. A., Mould, J. R., Stetson, P. B., Saha, A., Freedman, W. L. and Kennicutt, R. C. 2000b, *PASP*, 112, 177  
Freedman, W. L. *et al.* 2001, *ApJ*, April 10, in press, *astroph/0012376*  
Gibson, B. K., *et al.* 2000, *ApJ*, 529, 723  
Jha, S., *et al.* 1999, *ApJS*, 125, 73  
Kelson, D. D., *et al.* 2000, *ApJ*, 529, 768  
Kolb, E. W., & Turner, M. S. 1990, *The Early Universe*, Addison-Wesley, New York  
Madore, B. F., *et al.* 1999, *ApJ*, 515, 29  
Mould, J. R., *et al.* 2000, *ApJ*, 529, 786  
Perlmutter, S., *et al.* 1999, *ApJ*, 517, 565  
Reese, E. D., Mohr, J. J., Carlstrom, J. E., Joy, M., Grego, L., Holder, G. P., Holzapfel, W. L., Hughes, J. P., Patel, S. K., & Donahue, M. 2000, *ApJ*, 533, 38  
Riess, A. G., *et al.* 1998, *AJ*, 116, 1009  
Sandage, A. R., Saha, A., Tammann, G. A., Labhardt, L., Panagia, N., & Macchetto, F. D. 1996, *ApJ*, 460, 15  
Tanvir, N. R., Ferguson, H. C., & Shanks, T. 1999, *MNRAS*, 310, 175  
Udalski, A., Szymanski, M., Kubiak, M., Pietrzynski, G., Soszynski, I, Wozniak, P., & Zebrun, K. 1999, *Acta Astronomica*, 49, 201  
Williams, L. L. R., & Saha, P. 2000, *AJ*, 119, 439